

## Investigation of the rise time and damping of spin excitations in Ni<sub>81</sub>Fe<sub>19</sub> thin films

J. Wu, N. D. Hughes, J. R. Moore, and R. J. Hicken

Citation: *J. Appl. Phys.* **89**, 6692 (2001); doi: 10.1063/1.1357142

View online: <http://dx.doi.org/10.1063/1.1357142>

View Table of Contents: <http://jap.aip.org/resource/1/JAPIAU/v89/i11>

Published by the [American Institute of Physics](http://www.aip.org).

---

### Related Articles

Nanotube wall thickness dependent magnetization reversal properties of NiFe nanotubes

*J. Appl. Phys.* **113**, 024315 (2013)

Nb lateral Josephson junctions induced by a NiFe cross strip

*Appl. Phys. Lett.* **101**, 242601 (2012)

Phase stability and magnetic-field-induced martensitic transformation in Mn-rich NiMnSn alloys

*AIP Advances* **2**, 042181 (2012)

Field-induced lattice deformation contribution to the magnetic anisotropy

*J. Appl. Phys.* **112**, 103920 (2012)

Effects of DyHx and Dy<sub>2</sub>O<sub>3</sub> powder addition on magnetic and microstructural properties of Nd-Fe-B sintered magnets

*J. Appl. Phys.* **112**, 093912 (2012)

---

### Additional information on *J. Appl. Phys.*

Journal Homepage: <http://jap.aip.org/>

Journal Information: [http://jap.aip.org/about/about\\_the\\_journal](http://jap.aip.org/about/about_the_journal)

Top downloads: [http://jap.aip.org/features/most\\_downloaded](http://jap.aip.org/features/most_downloaded)

Information for Authors: <http://jap.aip.org/authors>

## ADVERTISEMENT



**AIP Advances**

Now Indexed in Thomson Reuters Databases

Explore AIP's open access journal:

- Rapid publication
- Article-level metrics
- Post-publication rating and commenting

# Investigation of the rise time and damping of spin excitations in Ni<sub>81</sub>Fe<sub>19</sub> thin films

J. Wu, N. D. Hughes, J. R. Moore, and R. J. Hicken<sup>a)</sup>

*School of Physics, University of Exeter, Stocker Road, Exeter EX4 4QL, United Kingdom*

The rise and damping of spin excitations in three Ni<sub>81</sub>Fe<sub>19</sub> films of thickness 50, 500, and 5000 Å have been studied with an optical pump–probe technique in which the sample is pumped with an optically triggered magnetic field pulse. The motion of the magnetization was described by the uniform mode solution of the Landau–Lifshitz–Gilbert equation. The rise time of the pulsed field within the film was smallest in the 50 Å sample and was generally greater when the pulsed field was perpendicular to the film plane. The damping constant was smallest in the 500 Å sample. The variations in the rise time and damping are attributed to the presence of eddy currents and structural disorder in the films. Under certain excitation conditions a second mode was observed in the 5000 Å sample which we believe to be a magnetostatic surface mode. © 2001 American Institute of Physics. [DOI: 10.1063/1.1357142]

Picosecond magnetic switching is being intensively studied so that it may be employed in future high speed data storage technology. The picosecond switching induced by a pulsed magnetic field has a precessional character that is sensitive to both the rise time of the pulsed field within the sample and the magnetic damping present. Magneto-optical pump–probe spectroscopy has emerged as a powerful tool with which to observe picosecond magnetization dynamics in thin films.<sup>1,2</sup> Using this technique we recently measured the field rise time and the damping parameter in a 500 Å Fe film.<sup>3</sup> In this article we investigate the variation of these quantities in polycrystalline Ni<sub>81</sub>Fe<sub>19</sub> films of thickness  $d = 50, 500, \text{ and } 5000 \text{ Å}$ .

Samples were prepared in a magnetron sputtering system, with base pressure of  $3 \times 10^{-7}$  Torr, at an Ar pressure of 3.5 mTorr. The Ni<sub>81</sub>Fe<sub>19</sub> was sputtered onto glass substrates and covered with a 6 nm layer of Al<sub>2</sub>O<sub>3</sub>. Longitudinal magneto-optical Kerr effect (MOKE) hysteresis loops revealed that the 50 and 500 Å films possessed a simple in-plane uniaxial anisotropy with hard axis saturation fields of 10 and 11 Oe, respectively. The 5000 Å film was isotropic within the film plane with a saturation field of 130 Oe. Alternating gradient magnetometer measurements showed that the magnetization of the 500 and 5000 Å films was close to the bulk value of 861 emu/cm<sup>3</sup>, while the magnetization of the 50 Å sample was  $296 \pm 26 \text{ emu/cm}^3$ .

In our time-resolved MOKE experiment the sample magnetization is pumped by the magnetic field generated by an optically triggered current pulse.<sup>2,3</sup> The samples are placed face down on a coplanar transmission line, shown in cross section in Fig. 1, and probed through the glass substrate with a 20 μm focused spot. The coplanar strips were perpendicular to the plane of incidence of the probe beam and a static field was applied either: (A) perpendicular to, or (B) in the plane of incidence. In this study the coplanar strips had a width and separation of 30 μm and a resistance of about 30 Ω/mm. The current in the strips was monitored with

an oscilloscope<sup>2</sup> and found to have a decay time of  $\tau = 1.5 \text{ ns}$ . From the measured current the peak magnetic field strength was deduced to be approximately 3 Oe immediately above the strips. The pumping field was modulated at about 200 Hz, by chopping the pump beam, and the probe signal was measured in a phase sensitive manner.

The measured Kerr rotation was compared with that predicted by a simple model. We first calculated the uniform mode solution of the Landau–Lifshitz–Gilbert equation for the thin film with in-plane uniaxial anisotropy and then calculated the instantaneous Kerr rotation by including contributions from both the longitudinal and polar Kerr effects.<sup>3</sup> In the present study we assumed that the pulsed field  $\mathbf{h}(t)$  within the sample had the form given in Eq. (1). The constant  $\tau_{\text{rise}}$  determines the rise time of the field pulse while  $\tau_{\text{refl}}$  determines the time of arrival of a negative pulse of relative amplitude  $R$ , which is due to a reflection of the current pulse on the coplanar transmission line.

$$\mathbf{h} = \begin{cases} \frac{e\mathbf{h}_0}{(e-1)} e^{-\tau_{\text{rise}}/t} (1 - e^{-t/\tau_{\text{rise}}}), & 0 \leq t \leq \tau_{\text{rise}} \\ \mathbf{h}_0 e^{-t/\tau}, & \tau_{\text{rise}} < t \leq \tau_{\text{refl}} \\ \mathbf{h}_0 [e^{-t/\tau} - R e^{-(t-\tau_{\text{refl}})/\tau}], & t > \tau_{\text{refl}} \end{cases} \quad (1)$$

Values of  $2.35 + 4.24i$  and  $0.0074 - 0.0046i$  were assumed for the values of the refractive index<sup>4</sup> and magneto-optic constant,<sup>5</sup> respectively. These are the values for nickel at the probe wavelength of 730 nm. The values for Ni<sub>81</sub>Fe<sub>19</sub> are not well known and so we do not attempt to reproduce the exact

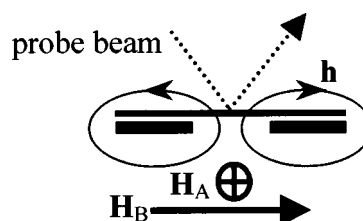


FIG. 1. The orientation of the static field  $\mathbf{H}$  is shown for the measurement geometries A and B. The coplanar transmission line, shown in cross section, carries a current that generates the azimuthal pulsed field  $\mathbf{h}$ .

<sup>a)</sup> Author to whom correspondence should be addressed; electronic mail: r.j.hicken@exeter.ac.uk

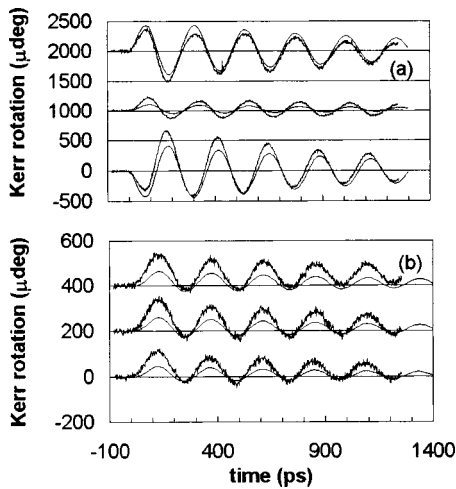


FIG. 2. The measured and simulated Kerr rotation are shown for the  $d = 500 \text{ \AA}$  sample, with  $H = 210 \text{ Oe}$ : (a) in geometry A and (b) in geometry B. In each case the middle trace corresponds to the probe spot position between the coplanar strips while the top and bottom traces correspond to positions above the two strips. The smooth simulated curves are discussed.

magnitude of the measured Kerr rotation. Instead we adjust the values of  $\tau_{\text{rise}}$ ,  $\tau_{\text{refl}}$ ,  $R$  and the damping constant  $\alpha$  to correctly reproduce the initial rise of the Kerr signal, and the phase and decay of successive oscillations.

The rectangular shaped samples were mounted on the transmission line with one edge parallel to the plane of incidence. The in-plane easy axis was oriented at  $53^\circ$  and  $40^\circ$  to the plane of incidence for the 50 and 500 Å samples, respectively. The probe spot was first scanned across the coplanar strips in geometry A with a static field sufficient to saturate

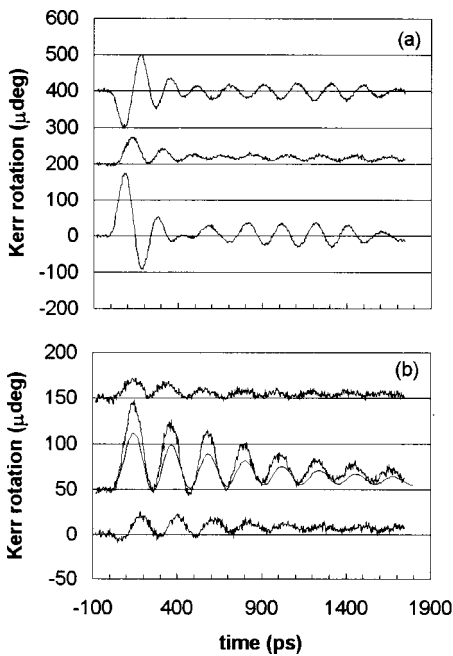


FIG. 3. The measured and simulated Kerr rotation are shown for the  $d = 5000 \text{ \AA}$  sample, with  $H = 216 \text{ Oe}$ : (a) in geometry A and (b) in geometry B. In each case the middle trace corresponds to the probe spot position between the coplanar strips while the top and bottom traces correspond to positions above the two strips. The smooth simulated curve in (b) is discussed.

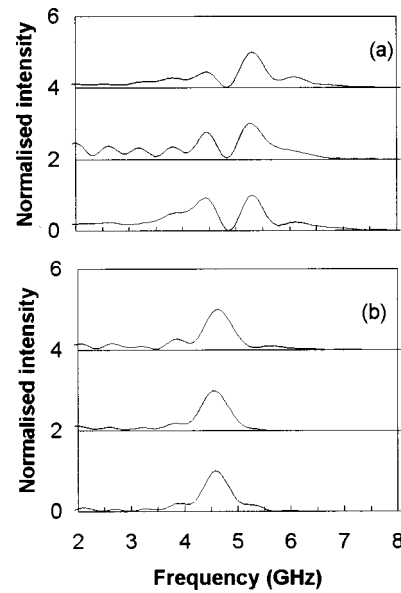


FIG. 4. The normalized power spectra of the data shown in Fig. 3 are plotted.

the sample. The amplitude of the Kerr signal exhibits two maxima which allow the positions of the coplanar strips to be identified. The signal from the 500 Å sample is shown in Fig. 2(a) at positions above and inbetween the coplanar strips. Since the orientation of the pumping field varies continuously above the strips and the probe spot has a finite diameter, the simulations are an average of 3 points that are each  $10 \mu\text{m}$  apart. The value of  $\tau_{\text{rise}}$  was found to be larger when the probe spot was between rather than above the strips. The 50 Å sample showed a similar behavior although the signal was more heavily damped. The data for the 5000 Å sample are shown in Fig. 3(a) and suggest the beating of two modes of different frequency. Measurements were also performed on the 500 and 5000 Å samples in geometry B, as shown in Fig. 2(b) and 3(b). A single value of  $\tau_{\text{rise}}$  was sufficient to simulate all the data in Fig. 2(b). In Fig. 3(b) the Kerr signal appears to contain only a single frequency component. Fourier transforms were taken of the data of Fig. 3. The power spectra shown in Fig. 4 confirm the presence of one and two modes in geometries B and A, respectively. The

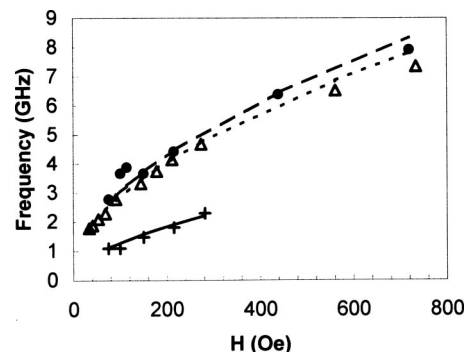


FIG. 5. FMR frequency is plotted as a function of static field  $H$  for  $d = 50 \text{ \AA}$ ; (+) continuous curve;  $500 \text{ \AA}$ ; ( $\Delta$ ) short dashed curve;  $5000 \text{ \AA}$  ( $\bullet$ ) long dashed curve. The curves assume the parameter values in Table I.

TABLE I. Parameter values used in modeling the time resolved MOKE data are shown. The letters A and B refer to the two measurement geometries.

| $d$ (Å)                    | 50        | 500                      | 5000       |
|----------------------------|-----------|--------------------------|------------|
| $M$ (emu/cm <sup>3</sup> ) | 296       | 800                      | 860        |
| $g$                        | 2.15      | 2.00                     | 2.11       |
| $H_{\text{sat}}$ (Oe)      | 10        | 11                       | 130        |
| $\tau_{\text{rise}}$ (ps)  | 10–40 (A) | 20–70 (A)<br>70 (B)      | 90 (B)     |
| $\tau_{\text{refl}}$ (ps)  | 205       | 95                       | 165        |
| $R$                        | 0.2       | 0.5                      | 0.2        |
| $\alpha$                   | 0.121 (A) | 0.0083 (A)<br>0.0076 (B) | 0.0129 (B) |

central trace in Fig. 3(b) was simulated to obtain values for  $\tau_{\text{rise}}$  and  $\alpha$ .

Measurements were made as a function of the static field value  $H$  in geometry A with the probe spot above one of the coplanar strips. The power spectra of the 50 and 500 Å samples showed single peaks which we identify as the uniform ferromagnetic resonance (FMR) mode. The 5000 Å sample yielded two major peaks and, as we will later justify, we identify the lower frequency peak as the uniform mode. The uniform mode frequencies have been plotted in Fig. 5. The curves were calculated from equations for the FMR frequency given in Ref. 4, using the parameter values shown in Table I. For the 50 Å sample the  $g$  factor was set to 2.15 and a perpendicular anisotropy field,  $H_{\perp} = 2.12$  kOe, was introduced in order to reduce the effective demagnetizing field  $4\pi M_{\text{eff}} = 4\pi M - H_{\perp}$ . Without this field an unphysically small  $g$  factor of about 1.5 was required to fit the curve to the data.

Figures 2 and 3 show that qualitatively different behavior occurs in the two measurement geometries. In geometry B the in-plane component of the pulsed field is parallel to the static field and so exerts no torque on the magnetization. As the probe spot is scanned, the shape of the curves and the values of  $\tau_{\text{rise}}$  and  $\alpha$  are unchanged. The amplitude of the response is proportional to the out of plane component of the pulsed field. In geometry A the shape of the curves changes as the probe spot is scanned. We attribute the variation of  $\tau_{\text{rise}}$  to eddy currents that delay the rise of the out of plane component of the pulsed field within the sample. The largest values of  $\tau_{\text{rise}}$  were obtained between the coplanar strips where the pulsed field lies perpendicular to the sample plane. Since the spatial distribution of the dynamical magnetization is very different in geometries A and B, the eddy current distributions are different and two somewhat different values of  $\alpha$  are observed for the 500 Å sample. Similar variations of  $\tau_{\text{rise}}$  and  $\alpha$  were found in Ref. 3. The values of  $\tau_{\text{rise}}$  increase with film thickness, suggesting the presence of eddy currents. The largest value of  $\alpha$  was obtained for the thinnest sample, perhaps because of structural disorder that also causes the room temperature magnetization to be reduced. Eddy current damping may again explain why the value of  $\alpha$  is larger for  $d = 5000$  Å than for  $d = 500$  Å. Since the three samples were placed at different positions above the transmission line some variation in the values of  $\tau_{\text{refl}}$  and  $R$  is not surprising.

In Fig. 4 the lower frequency mode in (a) has similar frequency to that in (b) and is identified as the uniform mode. The higher frequency mode in (a) is unlikely to be a standing spin wave mode with wave vector perpendicular to the sample plane. The excitation of such modes requires pinning of interfacial spins, for which we have no evidence, and a simple model of spin wave resonance<sup>6</sup> predicts a series of modes with spacings smaller than that observed. Instead we suggest that the higher frequency mode is a magnetostatic surface mode. Since the in-plane component of the pulsed field changes sign over a distance of 60  $\mu\text{m}$ , let us assume that the mode has a wavelength of 120  $\mu\text{m}$ , in which case  $kd = 0.026$ , where  $k$  is the magnitude of the in-plane wave vector. According to the Damon–Eshbach theory,<sup>7</sup> there is no surface mode when the wave vector is parallel to the static magnetization, and in the limit  $kd \ll 1$  the volume modes have the uniform mode frequency  $\omega_0$  given by

$$\left(\frac{\omega_0}{\gamma}\right)^2 = H(H + 4\pi M), \quad (2)$$

where  $\gamma = g \times \pi \times 2.80$  MHz/Oe. When the wave vector is perpendicular to the static magnetization, the volume mode frequency is given by Eq. (2) and the surface mode frequency  $\omega$  is given by

$$\left(\frac{\omega}{\gamma}\right)^2 = \left(\frac{\omega_0}{\gamma}\right)^2 + \frac{kd(4\pi M)^2}{2(1+kd)}. \quad (3)$$

From Eqs. (2) and (3) we calculate values of 4.56 and 5.80 GHz for the uniform and surface mode frequencies, respectively, in rough agreement with the peak positions shown in Fig. 4.

In summary, we have investigated the rise and damping of spin excitations in Ni<sub>81</sub>Fe<sub>19</sub> films of variable thickness. The rise time of the pulsed field within the film was found to be smallest in the 50 Å sample, while the damping constant was smallest in the 500 Å sample. The rise time is generally greater when the pulsed field is perpendicular to the film plane. The variations in the rise time and damping are attributed to the presence of eddy currents and to the presence of structural disorder in the thinnest sample. Finally we have also shown that the additional mode observed in the thickest sample is likely to be a magnetostatic surface mode.

The authors gratefully acknowledge the financial support of the UK Engineering and Physical Sciences Research Council.

<sup>1</sup>W. K. Hiebert, A. Stankiewicz, and M. R. Freeman, Phys. Rev. Lett. **79**, 1134 (1997); T. M. Crawford, T. J. Silva, C. W. Teplin, and C. T. Rogers, Appl. Phys. Lett. **74**, 3386 (1999); G. Ju, L. Chen, A. V. Nurmikko, R. F. C. Farrow, R. F. Marks, M. J. Carey, and B. A. Gurney, Phys. Rev. B **62**, 1171 (2000); B. Koopmans, M. van Kampen, J. T. Kohlhepp, and W. J. M. de Jonge, Phys. Rev. Lett. **85**, 844 (2000).

<sup>2</sup>R. J. Hicken and J. Wu, J. Appl. Phys. **85**, 4580 (1999).

<sup>3</sup>J. Wu, J. R. Moore, and R. J. Hicken, J. Magn. Magn. Mater. **222**, 189 (2000).

<sup>4</sup>Handbook of Chemistry and Physics, 75th ed., edited by D. R. Lide (Chemical Rubber Corp., Boca Raton, FL, 1994).

<sup>5</sup>G. S. Krinchik and V. A. Artem'ev, Sov. Phys. JETP **26**, 1080 (1968).

<sup>6</sup>A. H. Morrish, *The Physical Principles of Magnetism* (Krieger, Malabar, FL, 1983), Sec. 10.10.

<sup>7</sup>R. W. Damon and J. R. Eshbach, J. Phys. Chem. Solids **19**, 308 (1961).